International Journal of
Automotive Manufacturing and Materials（IJAMM）

Scilight

Article

Deterioration Analysis of Real-world SCR Catalysts in Diesel Vehicles

Tongliang Zhang [1,2,3], Yu Sun [3], Xusheng Xiang [4], Wenqing Ding [2,3], Zhen Chen [4], Caiyue Dong [4], Yating Li [3], Yulong Shan [3,*], Yunbo Yu [2,3], and Hong He [1,2,3]

[1] School of Rare Earths, University of Science and Technology of China, Hefei230026, China
[2] Ganjiang Innovation Academy, Chinese Academy of Sciences, Ganzhou341119, China
[3] State Key Joint Laboratory of Environment Simulation and Pollution Control, Research Center for Eco-Environmental Sciences, Chinese Academy of Sciences, Beijing100085, China
[4] Dongfeng Commercial Vehicle Co., Ltd., Shiyan100049, China
* Correspondence: ylshan@rcees.ac.cn
Received: 12 August 2024; Revised: 22 October 2024; Accepted: 24 October 2024; Published: 28 November 2024

Abstract: To investigate the real-world poisoning of Cu-SSZ-13 NH_3-SCR (Selective Catalytic Reduction with NH_3) catalysts in diesel vehicles, three used catalysts from vehicles that have traveled different distances were analyzed. The deterioration observed in these catalysts significantly differs from laboratory simulations due to the combined effect of multiple poisoning factors. The degree of catalyst deterioration is positively correlated not only with driving distance but also with the specific types of poisoning encountered. In real-world conditions, hydrothermal aging is not the primary poisoning factor. Instead, the main cause of Cu-SSZ-13 deactivation is the poisoning by chemical elements such as sulfur and iron. Sulfur poisoning reduces catalytic activity, and the regeneration of the catalyst depends on the species formed. This study reveals that the accumulation of chemical poisons is the primary reason for the deterioration of Cu-SSZ-13 catalysts in real-world conditions. Therefore, reducing toxic components in diesel engine exhaust is essential for maintaining catalyst performance.

Keywords: diesel emission; SCR catalysts; Cu-SSZ-13 zeolite; deterioration

1. Introduction

Diesel vehicles are essential to the global transportation industry due to their powerful engines and cost-effectiveness. However, NO_x emissions remain a significant issue, as diesel combustion is the primary power source for these vehicles [1]. Currently, NH_3-SCR technology is widely used for NO_x purification, with the NH_3-SCR catalyst as its core [2, 3]. Among commercial SCR catalysts, Cu-based small-pore zeolites, as represented with Cu-SSZ-13, serve as the primary coating materials, known for their efficient low-temperature catalytic performance and N_2 selectivity [4–7].

The stability of the SCR catalysts is essential for preventing excessive NO_x emissions. Numerous studies have focused on the poisoning effects on the Cu-SSZ-13 catalysts in the lab, primarily including hydrothermal aging process (HTA) and sulfur poisoning. In general, HTA process leads to the transformation of copper species from highly active state (Cu^{2+}-OH) into less active state (Cu^{2+}-2Z or CuO_x), accompanied with the deterioration of the zeolite framework structure [8–11]. Sulfur poisoning usually results in reversible ammonium sulfate poisoning, which severely inhibits low-temperature activity of the Cu-SSZ-13 but is easily regenerable [12]. Copper sulfate species are also formed after exposure to sulfur [13]. This should be seriously noted due to their irreversible poisoning effect on the SCR catalysts [14–16]. Besides, phosphorus and alkali metal poisoning have also been studied, mainly causing active copper species to transform into inert species such as Cu-P and CuO_x species, and resulting in the loss of acidic sites on the

Cu-SSZ-13 [17,18].

It is important to note that the aforementioned poisoning studies are mostly conducted through laboratory simulations with controlled ideal variables. However, in the actual operation of long-haul vehicles, catalyst faces more stringent and complex poisoning environments, where multiple poisoning species and high-temperature, high-humidity conditions coexist, far exceeding the anticipated pollution poisoning patterns [19]. For instance, the presence of SO_2 during hydrothermal aging greatly exacerbates the damage to active copper species and the collapse of the framework structure [20]. Therefore, evaluating catalyst poisoning in vehicles under real-world operating conditions is crucial for the emission control.

To assess the SCR performance of catalysts in real-world, this study conducts an evaluation and analysis of catalysts on in-use vehicles. The aim of this research is to investigate the poisoning of catalysts at the atomic level during operation in real-world and to provide theoretical guidance for policy formulation and emission control strategies.

2. Experimental Section

2.1. Catalyst Information

The integral Cu-SSZ-13 monolith NH_3-SCR catalyst in the exhaust aftertreatment system of the diesel vehicles have traveled different distances (100,000, 145,000 and 194,000 km) is taken out, which named Cat.-10, Cat.-14.5 and Cat.-19.4, respectively, and the catalyst coating on the surface of the integral catalyst is scraped off, with position (1) close to the center of the integral catalyst and position (2) close to the periphery of the integral catalyst. The scraped powder is ground and then tested.

2.2. Catalyst Evaluation

A fixed-bed quartz flow reactor was employed to determine the NH_3-SCR activities of the Cu-SSZ-13 catalysts. Samples of about 100 mg (40−60 mesh) were evaluated with a gas hourly space velocity (GHSV) of 200,000 h^{-1} and a total flow rate of 500 mL/min. The NH_3-SCR reaction conditions were controlled as follows: [NO] = 500 ppm, [NH_3] = 500 ppm, [O_2] = 5 vol.%, [H_2O] = 5 vol.%, N_2 balance. The NO, NO_2 and N_2O concentrations were monitored by an online Nicolet Is10 spectrometer. The NO_x conversion levels were calculated using the equation as follows:

$$NO_x \text{ conversion} = \frac{[NO_x]_{in} - [NO_x]_{out}}{[NO_x]_{in}} \times 100\%, \ (x = 1, 2) \quad (1)$$

2.3. Catalyst Characterizations

Powder X-ray diffraction (PXRD) patterns were recorded on a computerized Bruker D8 Advance diffractometer with Cu Kα (λ = 0.15406 nm) radiation at room temperature. The data were collected with 2θ ranging from 5° to 45° with the step size of 0.02°.

Scanning electron microscopy (SEM) was used to investigate the morphology of the Cu-SSZ-13 catalysts. High-resolution transmission electron microscopy (HRTEM) and Energy Dispersive Spectroscopy mapping (EDS mapping) were used to observe the morphology of the catalyst samples and the distribution of elements. The experimental images were obtained on a JEM2100PLUS microscope with an accelerating voltage of 200 kV.

H_2 temperature programmed reduction (H_2-TPR) analysis is used to investigate the distribution state and redox properties of Cu species in the Cu-SSZ-13 zeolite samples. This experiment was conducted on a Micromeritics AutoChem 2920 chemisorption analyzer. Prior to the experiment, the granular sample (100 mg) is pretreated at 500 °C for 1 h (heating rate of 10 °C/min) under a 20% O_2/N_2 atmosphere. After cooling to room temperature, Ar is introduced for purging. Finally, the atmosphere is switched to 10% H_2/Ar, and the temperature is increased to 900 °C (10 °C/min) after the baseline stabilizes. A TCD detector is used to detect the signal, thus resulting in the H_2 consumption curve.

Temperature-programmed desorption (TPD) experiments were conducted to investigate the content of surface adsorbed species on the catalyst samples. The sample was placed in a flow of N_2 and then heated at a ramp rate of 10 °C/min. The production of CO_2 and SO_2 was detected by a mass spectrometer.

The temperature programmed desorption of NH_3 (NH_3-TPD) experiment is used to investigate the

content and distribution of acidic sites on the catalyst samples. This experiment is conducted on a Fourier transform infrared spectrometer (Thermo Nicolet IS10). Prior to the experiment, the sample is pretreated at 500 °C for 30 min in a 10% O_2/N_2 atmosphere (heating rate of 10 °C/min). After the temperature is reduced to 100 °C, the 10% O_2/N_2 flow is turned off, and 500 ppm of NH_3 is introduced to the sample for continuous adsorption until saturation. Subsequently, the sample is purged with N_2 for 2 h and is heated from 100 °C to 700 °C (heating rate of 10 °C/min) to obtain the NH_3 desorption curve.

3. Results and Discussion

3.1. NH_3-SCR Performance of the Catalysts

To investigate the changes in the SCR catalysts on vehicles have traveled different distances, the coating powder of the obtained catalysts was subjected to standard NH_3-SCR activity evaluation and compared with the performance of unused fresh catalysts. As shown in Figure 1, the fresh catalyst exhibited excellent catalytic NO_x reduction performance. Catalysts of vehicles have traveled different distances showed varying degrees of activity decrease in both the low-temperature and high-temperature ranges. This indicates a loss of active sites in the catalyst and an increase in the NH_3 non-selective oxidation reaction [21]. Comparing to the deterioration of different samples, the Cat.-10 sample showed the least degree of deterioration, with only a slight decrease in the NH_3-SCR activity. In contrast, the Cat.-14.5 sample exhibited a significant decrease in the NH_3-SCR activity, which could be attributed to the poisoning of catalyst during the actual operation, leading to the deactivation of the Cu-SSZ-13 zeolite. Surprisingly, although the traveled distance of the Cat. -19.4 sample was the longest, the degree of decline in its catalytic performance was relatively low. Therefore, the degree of catalyst degradation in real-world does not entirely depend on the actual driving distance but is more influenced by the actual operating conditions.

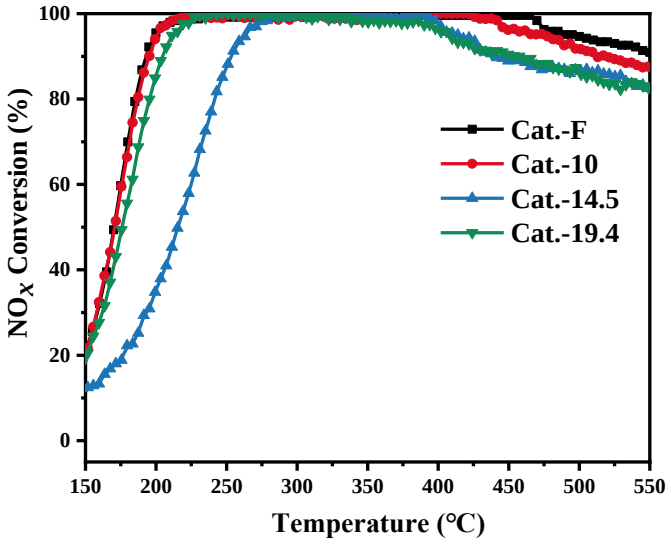

Figure 1. NH_3-SCR performances of the catalysts of vehicles have traveled different distances.

3.2. Morphology and Element Distribution of the Catalysts

Figure 2 presents the SEM images of the catalysts of vehicles with different driving distance at different scales. It can be seen that all the zeolites basically maintain their original state, but with the increase of actual operation distance, varying degrees of damage appear. The magnified SEM images show that the zeolite structure of all the samples has a certain degree of damage, with many small particulate species visible on the catalyst surface. These species may originate from fragments of the broken zeolite structure or possibly as a result of additives introduced during the slurry preparation process.

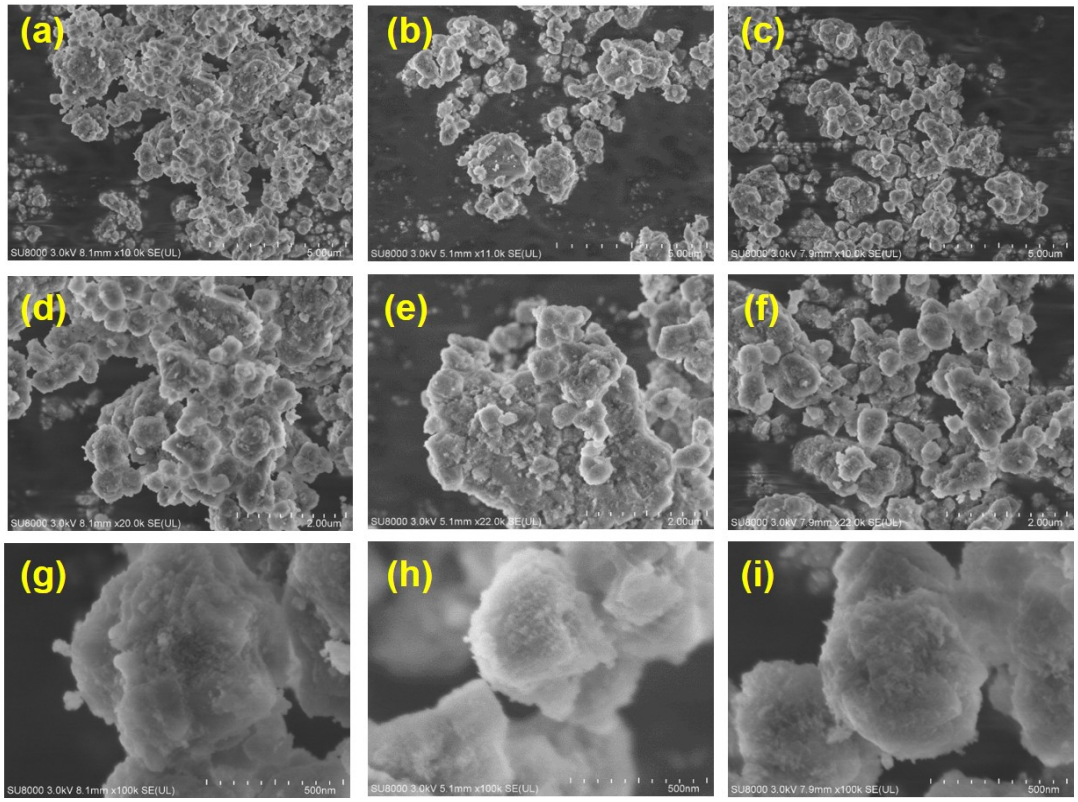

Figure 2. SEM images of the catalysts of vehicles have traveled different distances; Cat.-10 sample (**a**,**d**,**g**); Cat.-14.5 sample (**b**,**e**,**h**) and Cat.-19.4 sample (**c**,**f**,**i**).

The long-range ordered structures of the zeolites were further analyzed using XRD. As shown in Figure 3, prolonged operation did not alter the framework structure of the CHA zeolites obviously, but some impurity phases still appeared due to additives in the zeolite scraped off the cordierite substrate. By using BRUKER's TOPAS software, component separation of highly crystalline materials was performed. The actual proportions of zeolite material of samples Cat.-10, Cat.-14.5, and Cat.-19.4 were approximately 49%, 54%, and 63%, respectively (as listed in Table 1). Subsequent comparative experiments (activity, NH_3 storage, TPD, etc.) were normalized based on these component ratios.

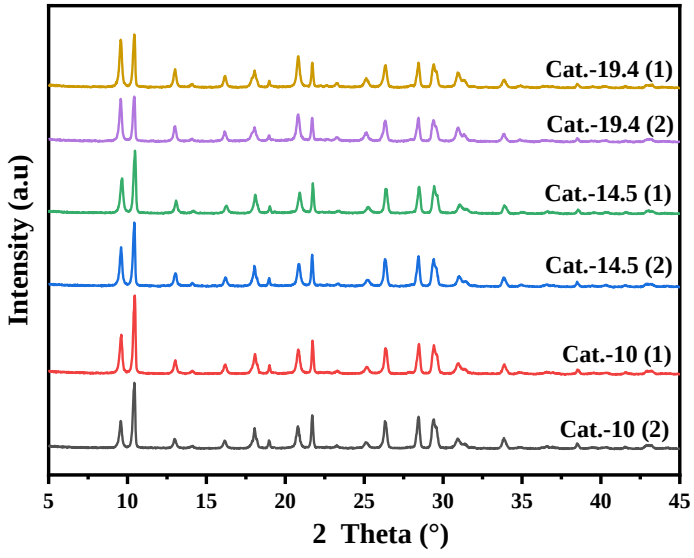

Figure 3. XRD patterns of the catalysts of vehicles have traveled different distances.

Table 1. The actual proportions of zeolite components in catalyst coating materials.

Samples	Proportion of Zeolite Components
Cat.-10 (1)	49.63%
Cat.-10 (2)	49.16%
Cat.-14.5 (1)	53.27%
Cat.-14.5 (2)	54.49%
Cat.-19.4 (1)	62.94%
Cat.-19.4 (2)	62.93%

In order to further analyze the elemental composition of these catalysts, we employed HRTEM and EDS mapping techniques (see Figure 4). The results indicate that in addition to the ordinary elements such as Cu, Si, Al, and O found in the zeolite and coating slurry additives, there are also other elements presented, such as non-metal components S and P as well as metal components Fe, Mg, and Cr. The presence of these elements may result from the interaction of the catalyst with various components in the diesel vehicle exhaust environment during operation. Generally, S primarily originates from diesel fuel, whereas P mainly comes from certain fuel additives. Metal elements such as Fe and Cr may come from the corrosion and shedding of the encapsulation structure in the after-treatment system, while alkali metals such as Mg and Ca (possibly present) may originate from ash and fuel additive components.

Moreover, in all three samples, the active copper species in the zeolites did not show significant aggregation, indicating that they remain highly dispersed after being used for different driving distances, demonstrating their excellent stability under real-world operation. Regarding poisoning species, Cat. -10 sample exhibited non-metal sulfur and phosphorus species and a large amount of metal-containing poisoning species (especially Fe and Mg species), which were aggregated into metal oxide clusters on the catalyst surface. Cat.-14.5 showed a great number of sulfur species, accompanied by small amounts of P, Fe, Mg, and Cr species. Although Cat. -19.4 had the longest driving distance, its surface species accumulation was relatively low. This could be due to its recent regeneration which led to the decomposition of volatile sulfur species, or may simply be attributed to the use of purer fuel that reduces the accumulation of poisoning species.

There are numerous studies that have reported the different effects of various poisoning species on the zeolite catalysts. For the sulfur poisoning, it primarily forms ammonium sulfate, copper sulfate and aluminium sulfate species on the zeolites. The ammonium sulfate species may cover active sites of the catalysts or cause pore blockage in the zeolites. Fortunately, the thermal decomposition temperature of ammonium sulfate is very low (~350 °C), enabling it to decompose during catalyst regeneration or normal operation period. This poisoning mechanism causes "reversible deactivation" of the zeolites, thus has a limited impact on the catalysts. Besides, the formation of copper sulfate species directly leads to the loss of Cu^{2+} active sites, reducing the NH_3-SCR reaction rate. Nevertheless, the decomposition temperature of copper sulfate species is above 600 °C, making it impossible to fully recover even after the "limited high-temperature regeneration" treatment, thus causing "irreversible deactivation" of the zeolite catalysts. In addition, the formation of aluminium sulfate species may cause the loss of Brønsted acid sites. [12,14,22–25]. In addition, P also combines with Cu species to form Cu-P species, which reduces the number of Cu active sites, and inhibits the reaction activity [18,26]. For Fe and Mg species, their accumulation amount and state may have different impacts on catalyst activity. Fe species can serve as active centers, which are especially beneficial for NH_3-SCR reaction at high temperatures. However, excessive Fe can also affect the state of Cu species, thus affecting SCR activity. Additionally, Fe_2O_3 increases the occurrence of non-selective ammonia oxidation reactions, resulting in a decrease in high-temperature NH_3-SCR activity [27]. Mg species, typically acting as alkaline metal poisoning species, can also affect the coordination state of Cu species, causing the aggregation of Cu species to CuO_x clusters, thus leading to framework collapse and NH_3 oxidation side reactions, thereby affecting SCR activity [17].

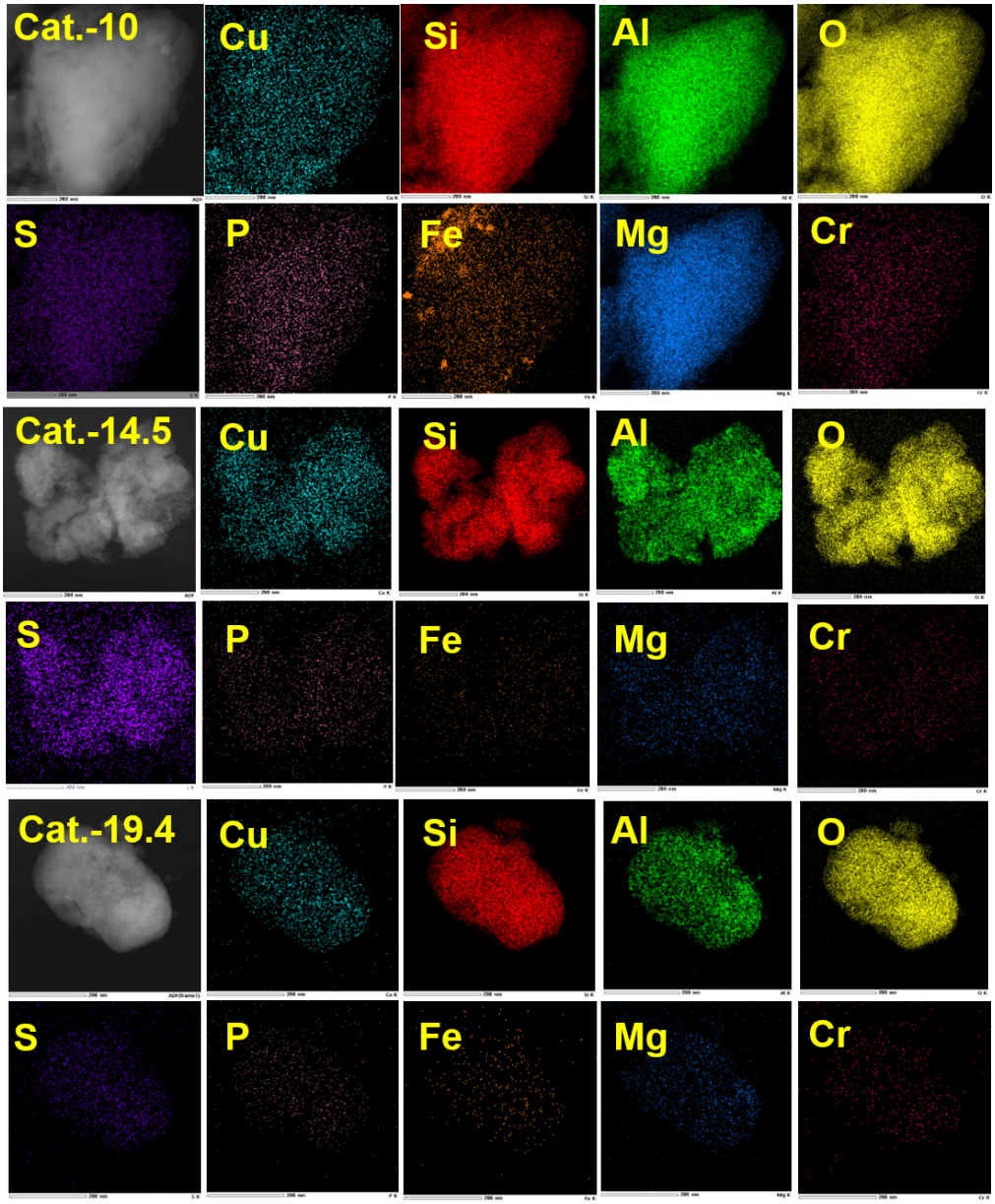

Figure 4. TEM images and EDS mapping analysis of the catalysts of vehicles have traveled different distances.

3.3. TPD analysis and Accumulated Species on Catalysts

The temperature-programmed desorption (TPD) experiment was used to further analyze the decomposable species deposited on the catalysts. The sample was placed in an N_2 stream for heating, and substances with mass numbers 64 and 44 were detected, which can be attributed to SO_2 and CO_2. Among them, SO_2 originates from the decomposition of sulfur-containing species, and CO_2 originates from the decomposition of carbon-containing functional groups. This indicates that sulfur species have accumulated on the catalyst and carbon deposition is present.

As can be seen from Figure 5a, SO_2 was almost undetectable in Cat.-10, only a small amount of SO_2 was detected in Cat.-19.4, while Cat.-14.5 exhibited significant sulfur dioxide desorption. Two desorption peaks were clearly observed in Cat.-14.5, which can be attributed to $CuSO_4$ and $Al_2(SO_4)_3$ species based on previous studies [23, 32]. No ammonium sulfate species were observed in the TPD experiments. As mentioned previously, ammonium sulphate tends to decompose during catalysts operation and regeneration. In addition, $CuSO_4$ species are very stable and require high temperatures (above 600 °C) to decompose, their formation thus leads to the irreversible deactivation of Cu active sites. Meanwhile, the formation of $Al_2(SO_4)_3$

species indicates that the Brønsted acid sites of the zeolite are also affected. The decomposition temperature of $Al_2(SO_4)_3$ species is higher than that of $CuSO_4$ species, thus also causing the irreversible deactivation of the zeolite [28]. Although it does not directly lead to the loss of Cu^{2+} active sites, by affecting the mobility of Cu^{2+} at low temperatures, $Al_2(SO_4)_3$ species can also reduce the low-temperature activity of Cu-SSZ-13. The excellent low-temperature NH_3-SCR performance of Cu-SSZ-13 relies on the cross-cage migration of Cu^{2+} in the form of copper-ammonia complexes. Therefore, the formation of $Al_2(SO_4)_3$ species will, on one hand, block the channels and increase the resistance to copper-ammonia complex migration; on the other hand, it will cause the loss of framework Al sites, resulting in a reduction in the number of Brønsted acid sites, thereby affecting the migration of copper-ammonia complexes too. This is mainly because the migration of copper-ammonia complexes needs to overcome the electrostatic attraction from the zeolite anionic framework and requires the counter-migration of H^+ (or H_3O^+ and NH_4^+) on Brønsted acid sites to balance the charge. Therefore, Brønsted acid sites can serve as "stepping stones" for the migration of copper-ammonia complexes during the low-temperature SCR reaction process [29]. This also explains the poor activity of Cat.-14.5 sample, as the formation of a large amount of $CuSO_4$ and $Al_2(SO_4)_3$ species leads to a reduction in active copper species, thus inhibiting the NH_3-SCR reaction rate. In contrast, only a small amount of SO_2 was detected in Cat.-19.4, indicating that only a limited amount of sulfur-containing species formed on it, thus resulting in a slight reduction in the SCR activity.

In addition, as shown in Figure 5b, a weak CO_2 signal was observed in all three samples, indicating that some carbon deposits were present on the catalyst during operation. However, despite the highest amount of carbon deposition being found in Cat.-10 Sample, its activity did not significantly decrease compared to the fresh sample, indicating that the current level of carbon deposition does not affect the SCR performance of the catalyst. The degree of sulfur poisoning is the determinant factor for catalyst deterioration.

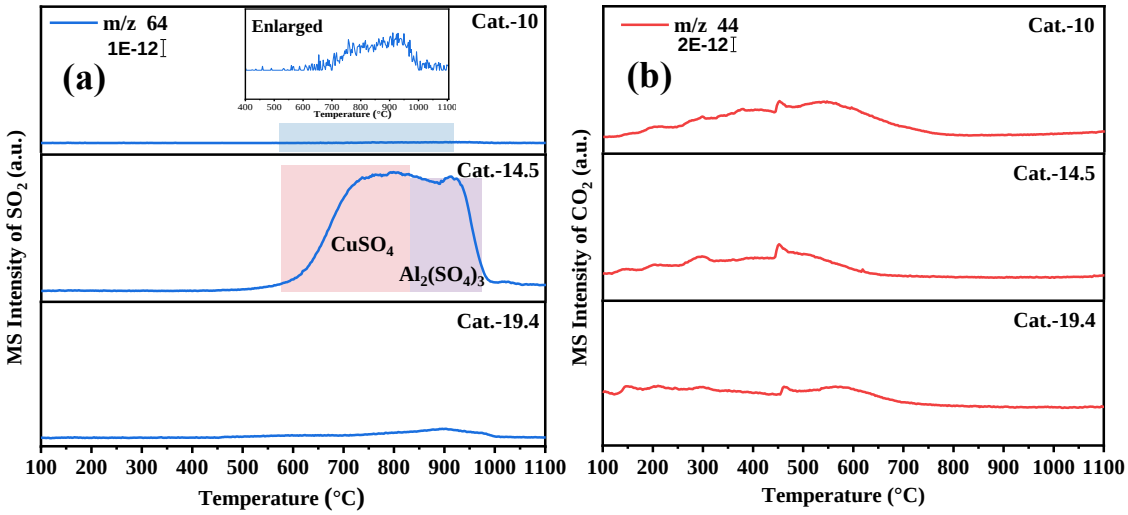

Figure 5. TPD results of the catalysts of vehicles have traveled different distances; (**a**) SO_2 MS signal and (**b**) CO_2 MS signal.

3.4. NH_3 Storage and Cu Specie Analysis of the Catalysts

To compare the changes in the strength and number of acidic sites on catalyst of vehicles have traveled different distances, NH_3-TPD was further applied to titrate the Lewis and Brønsted acidic sites in the samples. This analysis enabled the assessment of NH_3 storage performance of the obtained samples (as depicted in Figure 6), and the quantitative NH_3 storage results can be seen in Table 2. As shown in Figure 6, compared with the fresh sample (see Figure 6a), the NH_3 adsorption and desorption amounts of the three samples that have undergone actual vehicle operation significantly decreased. All tested samples exhibited three NH_3 desorption peaks, which, from low to high temperature, can be attributed to weak Brønsted acid sites, Lewis acid sites, and strong Brønsted acid sites, respectively [30,31]. The weak Brønsted acid sites mainly originate from the terminal hydroxyl groups of Si or Al and are related to the destruction of the framework structure.

For zeolites, Lewis acid sites are mainly from the active Cu^{2+} ions, but for these three samples, it may also come from added amorphous substances such as silicon-aluminum sol during the preparation of coating slurry [5]. Nevertheless, the Lewis acid sites of these actually operated catalysts also significantly decreased, especially in the Cat.-14.5 sample. This indicates a significant reduction in its active copper species, which may be due to the aggregation of CuO_x clusters or their combination with other toxic species (such as S), leading to the inability of active copper species to adsorb NH_3 molecules. Among the three samples, Cat.-10 still maintained the highest NH_3 adsorb content, thus exhibiting the highest SCR activity, while Cat.-14.5 Sample showed a significant reduction in NH_3 storage capacity, resulting in the poorest activity, which is consistent with the previous data.

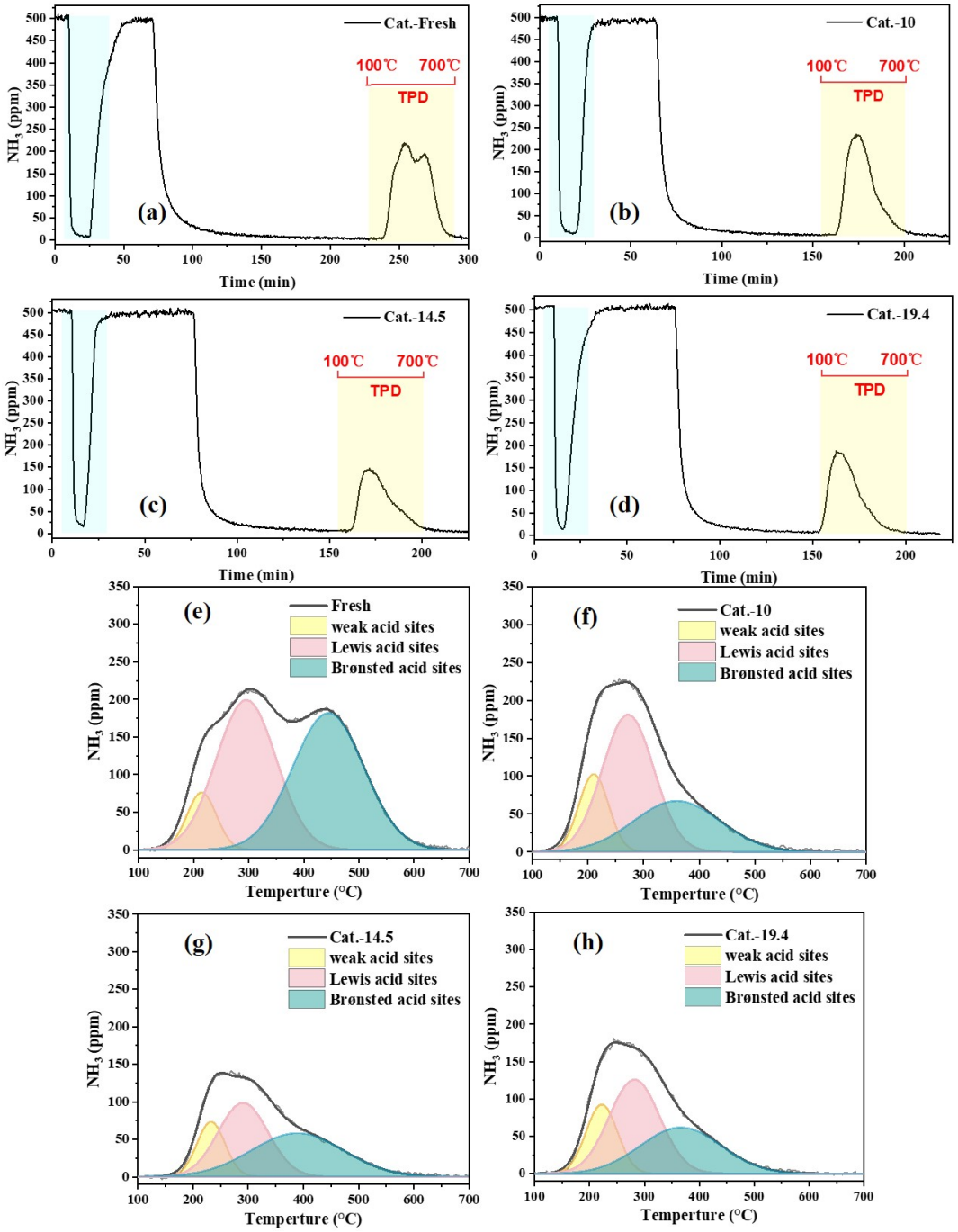

Figure 6. NH_3 storage analysis of the catalysts of vehicles have traveled different distances. (**a**–**d**) adsorption and desorption process; (**e**,**f**) split-peak plots of the desorption process.

Table 2. Quantification of desorbed NH_3 based on NH_3-TPD curve for different samples.

Sample	Adsorbed Amount (μmol/g)	Weak Acid Site (μmol/g)	Lewis Acid Sites (μmol/g)	Brønsted Acid Sites (μmol/g)	NH_3 Storage Capacity (μmol/g)
Fresh	2720	123	659	712	1495
Cat.-10	1615	166	509	316	991
Cat.-14.5	1152	112	271	292	675
Cat.-19.4	1291	161	351	277	789

H_2-TPR was also used to investigate the variations of Cu species in different zeolite samples, as shown in Figure 7. All three samples exhibited two H_2 reduction peaks in the temperature range of 200–400 °C, with peak center temperatures around 220 °C and 360 °C, which can be attributed to $[Cu(OH)]^+$-Al species located next to the eight-membered rings (8MRs) and Cu^{2+}-2Al species located at the six-membered ring (6MRs) windows of the Cu-SSZ-13 zeolite, respectively [5,32,33]. For the Cat.-10 sample with a lower degree of poisoning, no new reduction peaks were observed. This indicates that the copper species in this sample largely retain the form similar to the fresh sample, thus exhibiting the best catalytic activity. In contrast, new reduction peaks appeared at higher temperatures in the Cat.-14.5 and Cat.-19.4 samples, indicating the formation of new species. Among them, the signal of the new reduction peak is more pronounced in the most severely deteriorated Cat.-14.5 sample. Combined with the TPD analysis above, this suggests that the new peaks may be due to the decomposition of sulfates (copper sulfate) on the catalyst. Therefore, the H_2-TPR results further demonstrate that the impact of sulfur poisoning on Cu active sites is the key factor affecting the catalytic activity of the Cu-SSZ-13 zeolites. The Cu active sites in the Cat.-10 sample suffered the minimal damage, thus maintaining the highest NH_3-SCR catalytic activity.

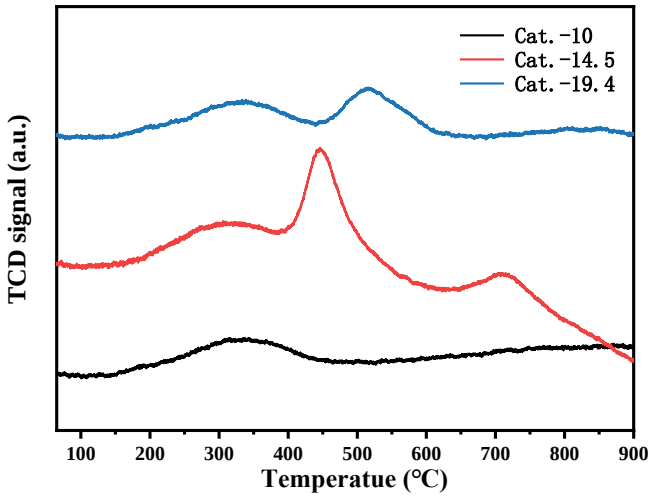

Figure 7. H_2-TPR profile of the catalysts of vehicles have traveled different distances.

3.5. SCR Performances of Regenerated Samples

From the above analysis, it can be concluded that sulfur poisoning has a decisive effect on the performance of the catalyst. High-temperature treatment can decompose sulfate species, thus enabling catalyst regeneration after sulfur poisoning [14,34]. This is also the main method for catalyst regeneration in actual vehicle operation. Therefore, we further investigated the NH_3-SCR catalytic performance of the regenerated vehicle catalysts have traveled different distances after high-temperature regeneration, and the results can be seen in Figure 8.

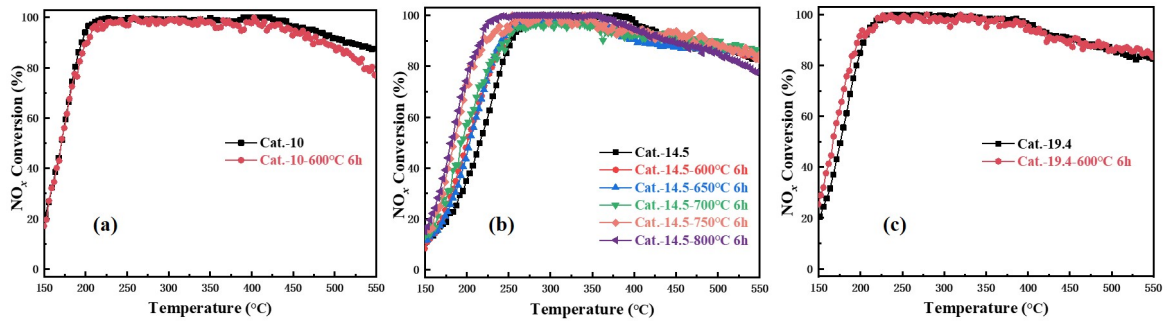

Figure 8. The NH_3-SCR performance of regenerated catalysts of vehicles have traveled different distances.

For the Cat.-10 sample, after high-temperature regeneration at 600 °C, the high-temperature activity of the catalyst slightly decreased. This may be due to the fact that the SCR activity of the Cat.-10 sample is close to that of the fresh sample, and the high-temperature regeneration leads to the aggregation of some copper species on its surface, which increases the non-selective oxidation of NH_3 [10]. For the Cat.-19.4 sample, high-temperature regeneration at 600 °C restored some of its low-temperature NH_3-SCR activity.

For the Cat.-14.5 sample, which had undergone the most severe degradation, the high-temperature regeneration at 600 °C also restored some of its low-temperature NH_3-SCR activity. With the increase in regeneration temperature, the activity continued to recover. Most of the SCR activity was restored when the temperature was raised to 800 °C, and the low-temperature NH_3-SCR activity was slightly lower than that of the fresh catalyst. This indicates that the regeneration temperature of 600 °C decomposed some of the metastable sulfate accumulated on the catalyst surface, reducing the degree of zeolite pore blockage and restoring its SCR performance to a certain extent. When the temperature increased to 800 °C, the stable sulfate species began to decompose, further restoring the SCR activity. However, it is not advisable to continue increasing the regeneration temperature above 800 °C because it may cause dealumination of the zeolite framework, leading to structural collapse and a subsequent decrease in NH_3-SCR activity.

4. Conclusion

The deterioration of the Cu-SSZ-13 catalyst in vehicles under real-world conditions significantly differs from the simulated laboratory conditions due to the combination of multiple poisoning factors. The degree of catalyst deterioration is not solely correlated with driving distance but also with the types of poisoning species present. In practical applications, hydrothermal aging is not the primary factor in catalyst deactivation; instead, poisoning by chemical elements such as sulfur and iron is more significant. Sulfur poisoning typically leads to decreased NH_3-SCR activity, and can often be reversed through various methods. While some sulfur species decompose easily, stable species such as $CuSO_4$ and $Al_2(SO_4)_3$ require regeneration at temperatures exceeding 800 °C, which may not be achievable during vehicle operation in real-world. Additionally, iron species formed from iron poisoning can act as active sites, contributing to certain SCR performances. This study reveals that cumulative chemical poisoning in real-world operation is the primary cause of SCR catalyst performance deterioration. Therefore, it is crucial to reduce toxic components in diesel exhaust to preserve catalyst efficacy.

Author Contributions: T. Z.: Data curation, Investigation, Formal analysis, Writing original draft, Writing—review & editing. Y. S.: Data curation, Investigation, Formal analysis, Writing—review & editing. X. X.: Data curation, Investigation, Validation. W. D.: Data curation, Investigation, Formal analysis, Validation. Z. C.: Validation. C. D.: Validation. Y.L.: Validation. Y.Y.: Validation. Y.S.: Conceptualization, Writing—review & editing, Project administration. H.H.: Writing—review & editing. All authors have read and agreed to the published version of the manuscript.

Funding: This work was financially supported by the National Key R&D Program of China (2023YFC3707201) and National Natural Science Foundation of China (52270112).

Institutional Review Board Statement: Not applicable.

Informed Consent Statement: Not applicable.

Data Availability: Statement: Not applicable.

Conflicts of Interest: The authors declare that they have no known competing financial interests or personal relationships that could have appeared to influence the work reported in this paper.

References

1. Jiang, Y.Q.; Ding, D.; Dong, Z.X.; Liu, S.C.; Chang, X.; Zheng, H.T.; Xing, J.; Wang, S.X. Extreme Emission Reduction Requirements for China to Achieve World Health Organization Global Air Quality Guidelines. *Environ. Sci. Technol.* **2023**, *57*, 4424–4433. https://doi.org/10.1021/acs.est.2c09164.
2. Bishop, G.A.; Haugen, M.J.; McDonald, B.C.; Boies, A.M. Utah Wintertime Measurements of Heavy-Duty Vehicle Nitrogen Oxide Emission Factors. *Environ. Sci. Technol.* **2022**, *56*, 1885 – 1893. https://doi. org/10.1021/acs. est. 1c06428.
3. Kong, H.; Lin, J.; Chen, L.; Zhang, Y.; Yan, Y.; Liu, M.; Ni, R.; Liu, Z.; Weng, H. Considerable Unaccounted Local Sources of $NO_{(x)}$ Emissions in China Revealed from Satellite. *Environ. Sci. Technol.***2 022**, *56*, 7131–7142. https://doi.org/10.1021/acs.est.1c07723.
4. Shan, Y.; He, G.; Du, J.; Sun ,Y.; Liu ,Z.; Fu ,Y.; Liu, F.; Shi, X.; Yu, Y.; He ,H. Strikingly distinctive NH**3**-SCR behavior over Cu-SSZ-13 in the presence of NO_2. *Nat. Commun.* **2022**, *13*, 4606. https://doi.org/10.1038/s41467-022-32136-z.
5. Sun, Y.; Fu, Y.; Shan, Y.; Du, J.; Liu, Z.; Gao, M.; Shi, X.; He, G.; Xue, S.; Han, X.; et al. Si/Al Ratio Determines the SCR Performance of Cu-SSZ-13 Catalysts in the Presence of NO_2. *Environ. Sci. Technol.* **2022**, *56*, 17946–17954. https://doi.org/10.1021/acs.est.2c03813.
6. Liang, J.; Mi, Y.; Song, G.; Peng, H.; Li, Y.; Yan, R.; Liu, W.; Wang, Z.; Wu, P.; Liu, F. Environmental benign synthesis of Nano-SSZ-13 via FAU trans-crystallization: Enhanced NH_3-SCR performance on Cu-SSZ-13 with nano-size effect. *J. Hazard. Mater.* **2020**, *398*, 122986. https://doi.org/10.1016/j.jhazmat.2020.122986.
7. Gao, F.; Mei, D.; Wang, Y.; Szanyi, J.; Peden, C.H. Selective Catalytic Reduction over Cu/SSZ-13: Linking Homo- and Heterogeneous Catalysis. *J. Am. Chem. Soc.* **2017**, *139*, 4935–4942. https://doi.org/10.1021/jacs.7b01128.
8. Song, J.; Wang, Y.; Walter, E.D.; Washton, N.M.; Mei, D.; Kovarik, L.; Engelhard, M.H.; Prodinger, S.; Wang, Y.; Peden, C.H.F.; et al. Toward Rational Design of Cu/SSZ-13 Selective Catalytic Reduction Catalysts: Implications from Atomic-Level Understanding of Hydrothermal Stability. *ACS Catal.* **2017**, *7*, 8214 – 8227. https://doi. org/10. 1021/acscatal.7b03020.
9. Zhang, Y.; Peng, Y.; Li, J.; Groden, K.; McEwen, J.-S.; Walter, E.D.; Chen, Y.; Wang, Y.; Gao, F. Probing Active-Site Relocation in Cu/SSZ-13 SCR Catalysts during Hydrothermal Aging by In Situ EPR Spectroscopy, Kinetics Studies, and DFT Calculations. *ACS Catal.* **2020**, *10*, 9410–9419. https://doi.org/10.1021/acscatal.0c01590.
10. Shan, Y.; Du, J.; Yu, Y.; Shan, W.; Shi, X.; He, H. Precise control of post-treatment significantly increases hydrothermal stability of in-situ synthesized cu-zeolites for NH_3-SCR reaction. *Appl. Catal. B Environ.* **2020**, *266*, 118655. https://doi.org/10.1016/j.apcatb.2020.118655.
11. Kim, Y.J.; Lee, J.K.; Min, K.M.; Hong, S.B.; Nam, I.-S.; Cho, B.K.Hydrothermal stability of CuSSZ13 for reducing NO_x by NH_3. *J. Catal.* **2014**, *311*, 447–457. https://doi.org/10.1016/j.jcat.2013.12.012.
12. Du, J.; Shi, X.; Shan, Y.; Xu, G.; Sun, Y.; Wang, Y.; Yu, Y.; Shan, W.; He, H. Effects of SO_2 on Cu-SSZ-39 catalyst for the selective catalytic reduction of NO_x with NH_3. *Catal. Sci. Technol.* **2020**, *10*, 1256–1263. https://doi.org/10.1039/c9cy02186h.
13. Qiu, Y.; Fan, C.; Sun, C.; Zhu, H.; Yi, W.; Chen, J.; Guo, L.; Niu, X.; Chen, J.; Peng, Y.; et al. New Insight into the In Situ SO_2 Poisoning Mechanism over Cu-SSZ-13 for the Selective Catalytic Reduction of NO_x with NH_3. *Catalysts* **2020**, *10*, 1391. https://doi.org/10.3390/catal10121391.
14. Hammershøi, P.S.; Jangjou, Y.; Epling, W.S.; Jensen, A.D.; Janssens T.V.W. *R*eversible and irreversible deactivation of Cu-CHA NH3-SCRcatalysts by SO_2 and SO_3. *Appl. Catal. B Environ.* **2018**, *226*, 38–45. https://doi.org/10.1016/j.apcatb.2017.12.018.
15. Shih, A.J.; Khurana, I.; Li, H.; González, J.; Kumar, A.; Paolucci, C.; Lardinois, T.M.; Jones, C.B.; Albarracin Caballero, J.D.; Kamasamudram, K.; et al. Spectroscopic and kinetic responses of Cu-SSZ-13 to SO_2 exposure and implications for NO_x selective catalytic reduction. *Appl. Catal. A Gen.* **2019**, *574*, 122–131. https://doi.org/10.1016/j.apcata.2019.01.024.
16. Wang, A.; Olsson, L. Insight into the SO**2**poisoning mechanism for NO_x removal by NH_3-SCR over Cu/LTA and Cu/SSZ-13. *Chem. Eng. J.* **2020**, *395*, 125048. https://doi.org/10.1016/j.cej.2020.125048.
17. Albert, K.B.; Fan, C.; Pang, L.; Chen, Z.; Ming, S.; Albert, T.; Li, T. The influence of chemical poisoning, hydrothermal aging and their co-effects on Cu-SAPO-34 catalyst for NO_x reduction by NH_3-SCR. *Appl. Surf. Sci.* **2019**, *479*, 1200–1211. https://doi.org/10.1016/j.apsusc.2019.02.120.
18. Chen J.; Shan Y.; Sun Y.; Ding W.; Xue S.; Han X.; Du J.; Yan Z.; Yu Y.; He H.Hydrothermal Aging Alleviates the Phosphorus Poisoning of Cu-SSZ-39 Catalysts for $NH_{(3)}$-SCR Reaction. *Environ. Sci. Technol.***2023**, *57*, 4113–4121. https://doi.org/10.1021/acs.est.2c08876.
19. Wu, Y.; Andana, T.; Wang, Y.; Chen, Y.; Walter, E.D.; Engelhard M.H.; Rappé K.G.; Wang Y.; Gao F.; Menon U.; et al. A comparative study between real-world and laboratory accelerated aging of Cu/SSZ-13 SCR catalysts. *Appl. Catal. B Environ.* **2022**, *318*, 121807. https://doi.org/10.1016/j.apcatb.2022.121807.
20. Zhang, Y.; Zhu, H.; Zhang, T.; Li, J.; Chen, J.; Peng, Y.; Li, J.Revealing the Synergistic Deactivation Mechanism of Hydrothermal Aging and $SO_{(2)}$ Poisoning on Cu/SSZ-13 under SCR Condition. *Environ. Sci. Technol.* **2022**, *56*, 1917–1926. https://doi.org/10.1021/acs.est.1c06068.

21. Xie, L.; Liu, F.; Ren, L.; Shi, X.; Xiao, F. S.; He, H. Excellent performance of one-pot synthesized Cu-SSZ-13 catalyst for the selective catalytic reduction of NO_x with NH_3. *Environ. Sci. Technol.* **2014**, *48*, 566–572. https://doi.org/10.1021/es4032002.
22. Hammershøi, P. S.; Jensen, A. D.; Janssens, T. V. W. Impact of SO_2-poisoning over the lifetime of a Cu-CHA catalyst for NH_3-SCR. *Appl. Catal. B Environ.* **2018**, *238*, 104–110. https://doi.org/10.1016/j.apcatb.2018.06.039.
23. Hammershøi, P. S.; Vennestrøm, P. N. R.; Falsig, H.; Jensen, A. D.; Janssens T. V. W. Importance of the Cu oxidation state for the SO_2-poisoning of a Cu-SAPO-34 catalyst in the NH*3*-SCR reaction. *Appl. Catal. B Environ.* **2018**, *236*, 377–383. https://doi.org/10.1016/j.apcatb.2018.05.038.
24. Wang, C.; Chen, Z.; Wang, J.; Wang, J.; Shen, M. Unraveling the nature of sulfur poisoning on Cu/SSZ-13 as a selective reduction catalyst. *J. Taiwan Inst. Chem. Eng.* **2021**, *118*, 38–47. https://doi.org/10.1016/j.jtice.2020.12.033.
25. Jangjou, Y.; Do, Q.; Gu, Y.; Lim, L.-G.; Sun, H.; Wang, D.; Kumar, A.; Li J.; Grabow, L.C.; Epling W.S.Nature of Cu Active Centers in Cu-SSZ-13 and Their Responses to SO_2 Exposure. *ACS Catal.* **2018**, *8*, 1325–1337. https://doi.org/10.1021/acscatal.7b03095.
26. Chen, Z.; Bian, C.; Guo, Y.; Pang, L.; Li, T. Efficient Strategy to Regenerate Phosphorus-Poisoned Cu-SSZ-13 Catalysts for the NH3-SCR of NOx: The Deactivation and Promotion Mechanism of Phosphorus. *ACS Catal.* **2021**, *11*, 12963–12976. https://doi.org/10.1021/acscatal.1c03752.
27. Sun, Y.; Shan, Y.; Ding, W.; Du, J.; Liu, Z.; Shi, X.; Ren, M.; Wang, Y.; Wang, X.; Yu, Y.; et al. Enhanced hydrothermal stability of Cu-SSZ-50 NH_3-SCR catalysts via the re-dispersion of introduced Fe upon hydrothermal processing. *Catal. Today* **2024**, *433*, 114690. https://doi.org/10.1016/j.cattod.2024.114690.
28. Su, W.; Li, Z.; Zhang, Y.; Meng, C.; Li, J.Identification of sulfate species and their influence on SCR performance of Cu/CHA catalyst. *Catal. Sci. Technol.* **2017**, *7*, 1523–1528. https://doi.org/10.1039/c7cy00302a.
29. Fu, Y.; Ding, W.; Lei, H.; Sun, Y.; Du, J.; Yu, Y.; Simon, U.; Chen, P.; Shan, Y.; He, G.; et al. Spatial Distribution of Bronsted Acid Sites Determines the Mobility of Reactive Cu Ions in the Cu-SSZ-13 Catalyst during the Selective Catalytic Reduction of $NO_{(x)}$ with $NH_{(3)}$. *J. Am. Chem. Soc.* **2024**, *146*, 11141 – 11151. https://doi. org/10.1021/jacs.3c13725.
30. Zhang, W.; Shen, M.; Wang, J.; Li, X.; Wang, J.; Shen, G.; Wang, C. Unraveling the nature of cerium on stabilizing Cu/SAPO-34 NH_3-SCR catalysts under hydrothermal aging at low temperatures. *J. Rare Earths* **2023**, *41*, 1551 – 1561. https://doi.org/10.1016/j.jre.2022.07.010.
31. Luo, J.; Kamasamudram, K.; Currier, N.; Yezerets, A. NH_3-TPD methodology for quantifying hydrothermal aging of Cu/SSZ-13 SCR catalysts. *Chem. Eng. Sci.* **2018**, *190*, 60–67. https://doi.org/10.1016/j.ces.2018.06.015.
32. Shan, Y.; Shi, X.; Yan, Z.; Liu, J.; Yu, Y.; He, H. Deactivation of Cu-SSZ-13 in the presence of SO_2 during hydrothermal aging. *Catal. Today* **2019**, *320*, 84–90. https://doi.org/10.1016/j.cattod.2017.11.006.
33. Du, J.; Han, S.; Huang, C.; Shan, Y.; Zhang, Y.; Shan, W.; He, H.Comparison of precursors for the synthesis of Cu-SSZ-39 zeolite catalysts for NH_3-SCR reaction. *Appl. Catal. B Environ.* **2023**, *338*, 123072. https://doi.org/10.1016/j.apcatb.2023.123072.
34. Mesilov, V.; Dahlin, S.; Bergman, S.L.; Xi, S.; Han, J.; Olsson, L.; Pettersson, L.J.; Bernasek, S.L. Regeneration of sulfur-poisoned Cu-SSZ-13 catalysts: Copper speciation and catalytic performance evaluation. *Appl. Catal. B Environ.***2021**, *299*, 120626. https://doi.org/10.1016/j.apcatb.2021.120626.